European Congress on Computational Methods in Applied Sciences and Engineering
ECCOMAS 2004
P. Neittaanmäki, T. Rossi, S. Korotov, E. Oñate, J. Périaux, and D. Knörzer (eds.)
Jyväskylä, 24–28 July 2004

ATOMIC MODELS OF DISLOCATIONS AND THEIR MOTION IN CUBIC CRYSTALS

A. Carpio*, and L. L. Bonilla†

*Departamento de Matemática Aplicada
Universidad Complutense de Madrid, 28040 Madrid, Spain
e-mail: ana_carpio@mat.ucm.es

† Escuela Politécnica Superior
Universidad Carlos III de Madrid, Avenida de la Universidad 30, 28911 Leganés, Spain
e-mail: bonilla@ing.uc3m.es

Key words: Atomic models, dislocations, cubic crystals, anisotropic elasticity.

Abstract. *A discrete model describing defects in crystal lattices and having the standard linear anisotropic elasticity as its continuum limit is proposed. The main ingredients entering the model are the elastic stiffness constants of the material and a dimensionless periodic function that restores the translation invariance of the crystal and influences the dislocation size. Explicit expressions are given for crystals with cubic symmetry: sc and fcc. Numerical simulations of this model illustrate static and moving edge and screw dislocations and describe their cores and profiles.*

1 INTRODUCTION

The advances of electronic microscopy allow imaging of atoms and can therefore be used to visualize the core of dislocations [1, 2], cracks [3] and other defects that control crystal growth and the mechanical, optical and electronic properties of the resulting materials [4]. Emerging behavior due to motion and interaction of defects might explain common but poorly understood phenomena such as friction [5]. Defects can be created in a controlled way by ion bombardment on reconstructed surfaces [6], which allows the study of effectively two dimensional (2D) single dislocations and dislocation dipoles. Other defects that are very important in multilayer growth are misfit dislocations [7]. At the nanoscale, many processes (for example, dislocation emission around nanoindentations [8]) involve the interaction of a few defects so close to each other that their core structure plays a fundamental role. To understand them, the traditional method of using information about the far field of the defects (extracted from linear elasticity) to infer properties of far apart defects reaches its limits. The alternative method of *ab initio* simulations is very costly and not very practical at the present time. Thus, it would be interesting to have systematic models of defect motion in crystals that can be solved cheaply, are compatible with elasticity and yield useful information about the defect cores and their mobility.

To see what these models of defects might be like, it is convenient to recall a few facts about dislocations. Consider for example an edge dislocation in a simple cubic (sc) lattice with a Burgers vector equal to one interionic distance in gliding motion, as in Fig. 1. The atoms above the xz plane glide over those below. Let us label the atoms by their position before the dislocation moves beyond the origin. Consider the atoms $(x_0, -a/2, 0)$ and $(x_0, a/2, 0)$ which are nearest neighbors before the dislocation passes them. After the passage of the dislocation, the nearest neighbor atoms are $(x_0, -a/2, 0)$ and $(x_0 - a, a/2, 0)$. This large excursion is incompatible with the main assumption under which linear elasticity is derived for a crystal structure [9]: the deviations of ions in a crystal lattice from their equilibrium positions are small (compared to the interionic distance), and therefore the ionic potentials entering the total potential energy of the crystal are approximately harmonic. One obvious way to describe dislocation motion is to simulate the atomic motion with the full ionic potentials. This description is possibly too costly. In fact, we know that the atomic displacements are small far from the dislocation core and that linear elasticity holds there. Is there an intermediate description that allows dislocation motion in a crystal structure and is compatible with a far field described by the corresponding anisotropic linear elasticity?

If we try to harmonize the continuum description of dislocations according to elasticity with an atomic description which is simply elasticity with finite differences instead of differentials, we face a second difficulty. The displacement vector of a static edge dislocation is multivalued. For example, its first component is $u_1 = a(2\pi)^{-1}[\tan^{-1}(y/x) + xy/(2(1-\nu)(x^2+y^2))]$ for the previously described edge dislocation (ν is the Poisson ratio) [1]. In elasticity, this fact does not cause any trouble because the physically relevant strain ten-

sor contains only derivatives of the displacement vector. These derivatives are continuous even across the positive x axis, where the displacement vector has a jump discontinuity $[u_1] = a$. If we consider an atomic model, and use differences instead of differentials, the difference of the displacement vector may still have a jump discontinuity across the positive x axis.

The previous difficulties have been solved in a simple model of edge dislocations and crowdions called the IAC model (interacting atomic chains model) proposed and studied by A.I. Landau and collaborators [10]. In the equations for the IAC model, the differences of the displacement vector are replaced by their sines. Unlike the finite differences, these sine functions are continuous across the positive x axis. Moreover, the equations remain unchanged if a horizontal chain of atoms slides an integer number of lattice periods a over another chain. Taking advantage of its simplicity, we have recently analyzed pinning and motion of edge dislocations in the IAC model [11].

In this paper, we propose a top-down approach to atomic models of dislocations in cubic crystals. Firstly, we discretize space along the primitive vectors defining the unit cell of the crystal. Secondly, we replace the gradient of the displacement vector in the strain energy by an appropriate periodic function of the discrete gradient, $g(D_j^+ u_i)$. Summing over all lattice sites, we obtain the potential energy of the crystal. Next, we find the equations of motion by the usual methods of classical mechanics. Far from the core of a defect, the discrete gradient approaches the continuous one. Then, provided the slope $g'(0)$ is one in the appropriate units, the spatially discrete equations of motion become those of the anisotropic elasticity. We illustrate our approach by constructing static and moving edge and screw dislocations in sc and fcc crystals.

The rest of the paper is organized as follows. The discrete models for simple cubic crystals are proposed in Section 2. Dislocations are then analyzed in Section 3: Static and moving screw and edge dislocations are numerically studied in Sections 3.1 and 3.2, respectively. In Section 4, we study dislocations in fcc cubic crystals, which requires formulating the equations of motion of the model in non-orthogonal coordinates. In fact, primitive vectors for fcc or bcc crystals are non-orthogonal, and the equations of motion describing these crystals should be invariant with respect to integer translations along non-orthogonal primitive vectors. To illustrate our ideas, we calculate numerically several relevant dislocations for gold (a fcc crystal). Section 5 contains our conclusions.

2 DISCRETE MODEL FOR A SIMPLE CUBIC LATTICE

To construct a spatially discrete model of a crystal having dislocations among its solutions, we shall start from the strain energy density for the appropriate anisotropic elasticity. In the case of cubic symmetry and considering infinitesimal displacements, the

strain energy density is [9]

$$W = \frac{1}{2} c_{ijkl} e_{ij} e_{kl}, \tag{1}$$

$$c_{ijkl} = \lambda\, \delta_{ij}\delta_{kl} + \mu\, (\delta_{ik}\delta_{jl} + \delta_{il}\delta_{jk}) + 2(C_{44} - \mu) \left(\frac{\delta_{ik}\delta_{jl} + \delta_{il}\delta_{jk}}{2} - \delta_{1i}\delta_{1j}\delta_{1k}\delta_{1l} - \delta_{2i}\delta_{2j}\delta_{2k}\delta_{2l} - \delta_{3i}\delta_{3j}\delta_{3k}\delta_{3l} \right), \tag{2}$$

provided the infinitesimal strain tensor is defined by the symmetric part of the distortion tensor w_{ij} [12]:

$$e_{ij} = \frac{w_{ij} + w_{ji}}{2}, \quad w_{ij} = \frac{\partial u_i}{\partial x_j}. \tag{3}$$

In all our equations, sum over repeated indices is always intended unless explicitly specified. u_i, $i = 1, 2, 3$, are the components of the displacement vector. λ and μ are related to the elastic stiffness constants C_{ij} [9] by

$$\lambda = C_{12}, \qquad \mu = \frac{C_{11} - C_{12}}{2}. \tag{4}$$

If $C_{44} = \mu = (C_{11} - C_{12})/2$, the strain energy density is isotropic, and λ and μ are the usual Lamé coefficients.

To obtain a discrete model for a sc crystal, we shall assume that space is discrete, so that $x = x_1 = la$, $y = x_2 = ma$, $z = x_3 = na$, where l, m and n are integer numbers. In Fig. 2(a), a is the side of the cubic cell, and therefore it is the primary unit of length. We shall measure the displacement vector in units of a, so that $u_i(x, y, z, t) = a\, u_i(l, m, n; t)$ and $u_i(l, m, n)$ is a nondimensional vector. Let D_j^+ and D_j^- represent the standard forward and backward difference operators, so that $D_1^{\pm} u_i(l, m, n; t) = \pm\, [u_i(l \pm 1, m, n; t) - u_i(l, m, n; t)]$, and so on. We shall define the *discrete* distortion tensor as

$$w_i^{(j)} = g(D_j^+ u_i), \tag{5}$$

where $g(x)$ is a periodic function of period one satisfying $g(x) \sim x$ as $x \to 0$. The strain energy for the discrete model is obtained by substituting the strain tensor:

$$e_{ij} = \frac{1}{2} \left(w_i^{(j)} + w_j^{(i)} \right) = \frac{g(D_j^+ u_i) + g(D_i^+ u_j)}{2}, \tag{6}$$

in Eq. (1). Once the displacement vector is known, the discrete strain energy density is a function of the point $W(\{u_i\}) = W(l, m, n)$, $(l, m, n) = (x, y, z)/a$, and the potential energy of the crystal is

$$V(\{u_i\}) = a^3 \sum_{l,m,n} W(l, m, n). \tag{7}$$

The definition (5) is useful when dislocations are present. In the far field of a dislocation, the differences of the nondimensional displacement vector are small, and therefore they approximate the components of the continuum distortion tensor in length scales much larger than a: $D_1^{\pm}u_i(l,m,n;t) = \pm\, a\,[u_i(l\pm 1,m,n;t) - u_i(l,m,n;t)]/a \approx \partial u_i/\partial x \ll 1$, and so on. In the far field of a dislocation, Eq. (5) yields $w_i^{(j)} \approx g(\partial u_i/\partial x_j) \approx \partial u_i/\partial x_j = w_{ij}$ because $g(x) \sim x$ as $x \to 0$. Then our proposed atomic model is compatible with continuum elasticity in the far field of dislocations. Near the dislocation core, our definition of discrete distortion tensor is free from the two problems of the simpler definition $w_i^{(j)} = D_j^+ u_i$, as mentioned in the Introduction. Firstly, the continuum displacement vector has a jump of size a across the axis directed along the Burgers vector of an edge dislocation with strength a. Correspondingly, the discrete displacement vector has a jump of size 1, but the discrete distortion tensor given by Eq. (5) is continuous. Secondly, consider a straight edge dislocation directed along the z axis, with Burgers vector of size a directed along the x axis and moving from left to right, as in Fig. 1. Let us label the atoms by their position before the dislocation moves beyond the origin. Consider the atoms $(x_0, -a/2, 0)$ and $(x_0, a/2, 0)$ which are nearest neighbors before the dislocation passes them. After the passage of the dislocation, the nearest neighbor atoms are $(x_0, -a/2, 0)$ and $(x_0 - a, a/2, 0)$. According to (5), $w_1^{(2)} = g(D_2^+ u_1) = g(D_2^+ u_1 + 1)$, and the discrete distortion tensor can be considered as a "difference" between neighboring atoms even when the passage of an edge dislocation has distorted the lattice.

The size of the dislocation core and its mobility depend on the function $g(x)$. In practice, the periodic function $g(x)$ should be fitted to data of the material at hand so as to have a good description of the defect core. However, in order to illustrate the theory and determine how the results depend on the shape of $g(x)$, we shall use in our calculations the odd piecewise linear function:

$$g(x) = \begin{cases} x, & |x| < \frac{1}{2} - \alpha, \\ \frac{(1-2\alpha)(1-2x)}{4\alpha}, & \frac{1}{2} - \alpha < x < \frac{1}{2} + \alpha, \end{cases} \tag{8}$$

which is periodically extended outside the interval $(\alpha - 1/2, \alpha + 1/2)$ for a given $\alpha \in (0, 1/2)$. Numerical simulations of the governing equations show that the dislocation core becomes smaller and the dislocation is harder to move if the interval of x in which $g'(x) > 0$ shrinks with respect to that in which $g'(x) < 0$.

To complete our description of an atomic model for sc crystals, we need to specify the equations of motion for the displacement vector. In the absence of dissipation and fluctuation effects the equations are:

$$\rho a^4\, \ddot{u}_i(l,m,n;t) = -\frac{1}{a}\,\frac{\partial V(\{u_k\})}{\partial u_i(l,m,n;t)}, \tag{9}$$

in which $\ddot{u}_i \equiv \partial^2 u_i/\partial t^2$. Equivalently,

$$M\,\ddot{u}_i(l,m,n;t) \;=\; -\frac{\partial}{\partial u_i(l,m,n;t)} \sum_{l',m',n'} W(l',m',n'), \tag{10}$$

provided we define $M = \rho a^2$, which has units of mass per unit length. Here the displacement vector is dimensionless, so that both sides of Eq. (10) have units of force per unit area. Eq. (10) is equivalent to

$$M\,\ddot{u}_i \;=\; \sum_{j,k,l} D_j^-[c_{ijkl}\,g'(D_j^+u_i)\,g(D_l^+u_k)]. \tag{11}$$

Let us now restore dimensional units to this equation, so that $u_i(x,y,z) = a\,u_i(x/a, y/a, z/a)$, then let $a \to 0$, use $\rho = M/a^2$ and that $g(x) \sim x$ as $x \to 0$. Then we obtain the equations of linear elasticity [12],

$$\rho\,\ddot{u}_i \;=\; \sum_{j,k,l} \frac{\partial}{\partial x_j}\left(c_{ijkl}\,\frac{\partial u_k}{\partial x_l}\right). \tag{12}$$

Thus the atomic model with conservative dynamics yields the Cauchy equations for elastic constants with cubic symmetry provided the components of the distortion tensor are very small (which holds in the dislocation far field).

3 Dislocation motion in sc crystals

In this Section, we shall find numerically pure screw and edge dislocations of our atomic model for sc symmetry and discuss their motion under appropriate applied stresses. The influence of the periodic function $g(x)$ on the size of the dislocation core and its mobility will also be considered. In all cases, the procedure to obtain numerically the dislocation from the atomic model is the same. We first solve the stationary equations of elasticity with appropriate singular source terms to obtain the *dimensional* displacement vector $\mathbf{u}(x,y,z) = (u_1(x,y,z), u_2(x,y,z), u_3(x,y,z))$ of the static dislocation *under zero applied stress*. This displacement vector yields the far field of the corresponding dislocation for the discrete model, which has the *nondimensional* displacement vector $\mathbf{U}(l,m,n) = \mathbf{u}(x/a, y/a, z/a)/a$. We use $\mathbf{U}(l,m,n)$ in the boundary and initial conditions for the discrete equations of motion of the atomic model.

3.1 Screw dislocations

The continuum displacement field of a dislocation, $\mathbf{u} = (u_1, u_2, u_3)$, can be calculated as a stationary solution of the anisotropic Navier equations with a singularity $\propto r^{-1}$ at the dislocation core and such that $\int_{\mathcal{C}}(d\mathbf{x}\cdot\nabla)\mathbf{u} = -\mathbf{b}$, where $\mathbf{b}$ is the Burgers vector and C is any closed curve encircling the dislocation line [12]. A pure screw dislocation along the z axis with Burgers vector $\mathbf{b} = (0,0,b)$ has a displacement vector $\mathbf{u} = (0,0,u_3(x,y))$ [1]. Then the strain energy density becomes $W = C_{44}\,|\nabla u_3|^2/2$, and the stationary equation of motion is $\Delta u_3 = 0$. Its solution corresponding to a screw dislocation is $u_3(x,y) = b\,(2\pi)^{-1}\tan^{-1}(y/x)$ [1]. The same symmetry considerations for Eq. (11) (conservative

dynamics) yield the following discrete equation for the z component of the nondimensional displacement $u_3(l,m;t)$:

$$M\,\ddot{u_3} \;=\; C_{44}\,\{D_1^-[g(D_1^+u_3)\,g'(D_1^+u_3)] + D_2^-[g(D_2^+u_3)\,g'(D_2^+u_3)]\}. \tag{13}$$

Numerical solutions of Eq. (13) show that a static screw dislocation moves if an applied shear stress surpasses the static Peierls stress, $|F| < F_{cs}$, but that a moving dislocations continues doing so until the applied shear stress falls below a lower threshold F_{cd} (dynamic Peierls stress); see Ref. [11] for a similar situation for edge dislocations. To find the static solution of this equation corresponding to a screw dislocation, we could minimize an energy functional. However, it is more efficient to solve the following overdamped equation:

$$\beta\,\dot{u_3} \;=\; C_{44}\,\{D_1^-[g(D_1^+u_3)\,g'(D_1^+u_3)] + D_2^-[g(D_2^+u_3)\,g'(D_2^+u_3)]\}. \tag{14}$$

The stationary solutions of Eqs. (13) and (14) are the same, but the solutions of (14) relax rapidly to the stationary solutions if we choose appropriately the damping coefficient β. We solve Eq. (14) with initial condition $u_3(l,m;0) = U_3(l,m) \equiv b\,(2\pi a)^{-1}\tan^{-1}(m/l)$, and with boundary conditions $u_3(l,m;t) = U_3(l,m) + F\,m$ at the upper and lower boundaries of our lattice (F is an applied dimensionless stress with $|F| < F_{cs}$). Then the solution of Eq. (14) relaxes to a static screw dislocation $u_3(l,m)$ with the desired far field. If $F = 0$, Figure 3 shows the helical structure adopted by the deformed lattice $(l, m, n + u_3(l,m))$ for for the asymmetric piecewise linear $g(x)$ of Eq. (8). The width of the dislocation core depends on C_{44} and on $g(x)$. Numerical solutions show that there may be coefficients with $g'(x) < 0$ in (13) or (14) at the core of a dislocation [11]. Thus the size of the dislocation core and the dislocation mobility depend on the shape of $g(x)$, precisely on the width of the interval of x for which $g'(x) < 0$. As this interval shrinks, the size of the core region decreases and the dislocation becomes harder to move. For practical use, the function $g(x)$ should be chosen so as to fit the characteristics of the material at hand.

The motion of a pure screw dislocation is somewhat special because its Burgers vector is parallel to the dislocation line. Any plane containing the Burgers vector can be a glide plane. Under a shear stress $F > F_{cs}$ directed along the y direction, a screw dislocation moves on the glide plane xz. A moving screw dislocation has the structure of a discrete traveling wave in the direction x, with far field $u_3(l - ct, m) + Fm$; $c = c(F)$ is the dislocation speed. This is similar to the case of edge dislocations in the simple IAC model [10], as discussed in [11] where the details of the analysis can be looked up.

3.2 Edge dislocations

To analyze edge dislocations in the simplest case, we consider a cubic crystal with planar discrete symmetry, so that $\mathbf{u}(l,m;t) = (u_1(l,m;t), u_2(l,m;t), 0)$ is independent of $z = na$, and ignore fluctuations. We assume that $C_{44} = (C_{11} - C_{12})/2$, so that the material is isotropic.

To find the stationary edge dislocation of the discrete model, we first have to write the corresponding stationary edge dislocation of isotropic elasticity. An edge dislocation

directed along the z axis (dislocation line), and having Burgers vector $(b,0,0)$ has a displacement vector $\mathbf{u} = (u_1(x,y), v_2(x,y), 0)$ with a singularity $\propto r^{-1}$ at the core and satisfying $\int_{\mathcal{C}}(d\mathbf{x}\cdot\nabla)\mathbf{u} = -(b,0,0)$, for any closed curve $\mathcal{C}$ encircling the z axis. It satisfies the planar stationary Navier equations (12) with a singular source term:

$$\Delta\mathbf{u} + \frac{1}{1-2\nu}\nabla(\nabla\cdot\mathbf{u}) = -(0,b,0)\,\delta(r). \tag{15}$$

Here $r = \sqrt{x^2+y^2}$ and $\nu = \lambda/[2(\lambda+\mu)]$ is the Poisson ratio; cf. page 114 of Ref. [12]. The appropriate solution is (cf. Ref. [1], pag. 57)

$$\begin{aligned} u_1 &= \frac{b}{2\pi}\left[\tan^{-1}\left(\frac{y}{x}\right) + \frac{xy}{2(1-\nu)(x^2+y^2)}\right], \\ u_2 &= \frac{b}{2\pi}\left[-\frac{1-2\nu}{4(1-\nu)}\,\ln\left(\frac{x^2+y^2}{b^2}\right) + \frac{y^2}{2(1-\nu)(x^2+y^2)}\right]. \end{aligned} \tag{16}$$

Eqs. (16) yield the nondimensional displacement vector $\mathbf{U}(l,m) = (u_1(la,ma)/a, u_2(la,ma)/a, 0)$, which will be used to find the stationary edge dislocation of the discrete equations of motion. For this planar configuration, the conservative equations of motion (11) become

$$\begin{aligned} M\,\ddot{u}_1 &= C_{11}\,D_1^-[g(D_1^+u_1)\,g'(D_1^+u_1)] + C_{12}\,D_1^-[g(D_2^+u_2)\,g'(D_1^+u_1)] \\ &\quad + C_{44}\,D_2^-\{[g(D_2^+u_1) + g(D_1^+u_2)]\,g'(D_2^+u_1)\}, \qquad (17) \\ M\,\ddot{u}_2 &= C_{11}\,D_2^-[g(D_2^+u_2)\,g'(D_2^+u_2)] + C_{12}\,D_2^-[g(D_1^+u_1)\,g'(D_2^+u_2)] \\ &\quad + C_{44}\,D_1^-\{[g(D_1^+u_2) + g(D_2^+u_1)]\,g'(D_1^+u_2)\}. \qquad (18) \end{aligned}$$

To find the stationary edge dislocation corresponding to these equations, we set $C_{44} = (C_{11}-C_{12})/2$ (isotropic case), and replace the inertial terms $M\ddot{u}_1$ and $M\ddot{u}_2$ by $\beta\dot{u}_1$ and $\beta\dot{u}_2$, respectively. The resulting overdamped equations,

$$\begin{aligned} \beta\,\dot{u}_1 &= C_{11}\,D_1^-[g(D_1^+u_1)\,g'(D_1^+u_1)] + C_{12}\,D_1^-[g(D_2^+u_2)\,g'(D_1^+u_1)] \\ &\quad + C_{44}\,D_2^-\{[g(D_2^+u_1) + g(D_1^+u_2)]\,g'(D_2^+u_1)\}, \qquad (19) \\ \beta\,\dot{u}_2 &= C_{11}\,D_2^-[g(D_2^+u_2)\,g'(D_2^+u_2)] + C_{12}\,D_2^-[g(D_1^+u_1)\,g'(D_2^+u_2)] \\ &\quad + C_{44}\,D_1^-\{[g(D_1^+u_2) + g(D_2^+u_1)]\,g'(D_1^+u_2)\}, \qquad (20) \end{aligned}$$

have the same stationary solutions as Eqs. (17) and (18). We solve Eqs. (19) and (20) with initial condition $\mathbf{u}(l,m;0) = \mathbf{U}(l,m)$ given by Eqs. (16), and with boundary conditions $\mathbf{u}(l,m;t) = \mathbf{U}(l,m) + F\,(m,0,0)$ at the upper and lower boundaries of the lattice (F is a dimensionless applied shear stress). If $|F| < F_{cs}$ (F_{cs} is the static Peierls stress for edge dislocations), the solution of Eqs. (19) and (20) relaxes to a static edge dislocation $(u_1(l,m), u_2(l,m), 0)$ with the appropriate continuum far field.

In our numerical calculations of the static edge dislocation, we use the elastic constants of tungsten (which is an isotropic bcc crystal), $C_{11} = 521.0$ GPa, $C_{12} = 201.0$ GPa, $C_{44} = 160.0$ GPa ($C_{11} = C_{12} + 2C_{44}$) [2]. This yields $\nu = 0.278$. Figure 1 shows the structure adopted by the deformed lattice $(l + u_1(l,m), m + u_2(l,m))$ when $\nu = 0.278$. The width of the dislocation core depends on the Poisson ratio ν and on the shape of $g(x)$. The profiles of the displacement vector are shown in Figure 4 for the asymmetric piecewise linear function $g(x)$. Numerical solutions show that the size of the dislocation core and the dislocation mobility depend on the shape of $g(x)$ in the same manner as they did for screw dislocations. As the interval of x for which $g'(x) < 0$ shrinks, the size of the core region decreases and the dislocation becomes harder to move.

The glide motion of edge dislocations occurs on the glide plane defined by their Burgers vector and the dislocation line, and in the direction of the Burgers vector. In our case, a shear stress in the direction y, will move the dislocation in the direction x. For conservative or damped dynamics, the applied shear stress has to surpass the static Peierls stress to depin a static dislocation, and a moving dislocation propagates provided the applied stress is larger than the dynamic Peierls stress (smaller than the static one) [11]. As $\alpha < 1/4$ in Eq. (8) decreases, the static Peierls stress increases, thereby rendering the dislocation less mobile. A moving dislocation is a discrete traveling wave advancing along the x axis, and having far field $(u_1(l - ct, m) + Fm, u_2(l - ct, m))$. The analysis of depinning and motion of planar edge dislocations follows that explained in Ref. [11] with technical complications due to our more complex discrete model.

4 ELASTICITY IN A NON-ORTHOGONAL BASIS: THE CASE OF FCC METALS

As shown in Fig. 2(b), the primitive vectors of the unit cell are not orthogonal for a fcc crystal. To find a discrete model for such a crystal, we should start by writing the strain energy density in a non-orthogonal vector basis, a_1, a_2, a_3, defined by

$$a_1 = \frac{a}{2}(1,1,0),\ a_2 = \frac{a}{2}(1,0,1),\ a_3 = \frac{a}{2}(0,1,1), \tag{21}$$

in terms of the usual orthonormal vector basis e_1, e_2, e_3 determined by the cube sides of length a. Let x_i denote coordinates in the basis e_i, and let x'_i denote coordinates in the basis a_i. Notice that the x_i have dimensions of length while the x'_i are dimensionless. The matrix $T = (a_1, a_2, a_3)$ whose columns are the coordinates of the new basis vectors in terms of the old orthonormal basis can be used to change coordinates as follows:

$$x'_i = T^{-1}_{ij} x_j,\ x_i = T_{ij} x'_j. \tag{22}$$

Similarly, the displacement vectors in both basis are related by

$$u'_i = T^{-1}_{ij} u_j,\ u_i = T_{ij} u'_j, \tag{23}$$

and partial derivatives obey

$$\frac{\partial}{\partial x_i'} = T_{ji}\frac{\partial}{\partial x_j},\ \frac{\partial}{\partial x_i} = T_{ji}^{-1}\frac{\partial}{\partial x_j'}. \tag{24}$$

Then the strain energy density $W = (1/2)c_{iklm}e_{ik}e_{lm}$ can be written as

$$W = \frac{1}{2}\,c_{ijlm}\frac{\partial u_i}{\partial x_j}\frac{\partial u_l}{\partial x_m} = \frac{1}{2}\,c'_{rspq}\frac{\partial u'_r}{\partial x'_s}\frac{\partial u'_p}{\partial x'_q}, \tag{25}$$

where the new elastic constants are:

$$c'_{rspq} = c_{ijlm}T_{ir}T_{sj}^{-1}T_{lp}T_{qm}^{-1}. \tag{26}$$

Notice that the elastic constants have the same dimensions in both the orthogonal and the non-orthogonal basis. To obtain a discrete model, we shall consider that the dimensionless displacement vector u_i' depends on dimensionless coordinates x_i' that are integer numbers $u_i' = u_i'(l,m,n)$. As in Section 2, we replace the distortion tensor (gradient of the displacement vector) by a periodic function of the corresponding forward difference, $w_i^{(j)} = g(D_j^+u_i')$. As in Eq. (6), g is a periodic function with $g'(0) = 1$ and period 1. The discretized strain energy density is

$$W(l,m,n) = \frac{1}{2}\,c'_{rspq}g(D_s^+u_r')\,g(D_q^+u_p'). \tag{27}$$

The function g may be fitted to experimental o molecular dynamics data, but, to illustrate the theory, we have chosen the piecewise linear function (8) in the numerical results presented in this paper. The elastic constants c'_{rspq} can be calculated in terms of the Voigt stiffness constants for a cubic crystal, C_{11}, C_{44} and C_{12}. Eq. (5) yields $c_{ijlm} = C_{44}(\delta_{il}\delta_{jm} + \delta_{im}\delta_{lj}) + C_{12}\delta_{ij}\delta_{lm} - H(\delta_{1i}\delta_{1j}\delta_{1l}\delta_{1m} + \delta_{2i}\delta_{2j}\delta_{2l}\delta_{2m} + \delta_{3i}\delta_{3j}\delta_{3l}\delta_{3m})$, where $H = 2C_{44} + C_{12} - C_{11}$ measures the anisotropy of the crystal. Then Eq. (26) provides the tensor c'_{rspq}. The elastic energy can be obtained from W by means of Eq. (7), and the conservative equations of motion (9) are then

$$\rho a^3\,\frac{\partial^2 u_i'}{\partial t^2} = -T_{iq}^{-1}T_{pq}^{-1}\frac{\partial V}{\partial u_p'}.$$

Together with Eqs. (7) and (27), these equations yield

$$\rho\,\frac{\partial^2 u_i'}{\partial t^2} = T_{iq}^{-1}T_{pq}^{-1}D_j^-[c'_{pjrs}\,g'(D_j^+u_p')\,g(D_s^+u_r')]. \tag{28}$$

Now we can analyze the motion of dislocations. The initial and boundary data for the numerical simulations are constructed from the far fields of dislocations in anisotropic elasticity. To calculate the elastic far field of any straight dislocation, we shall follow the

method explained in Chapter 13 of Hirth and Lothe's book [2]. Firstly, we determine the elastic constants in an orthonormal coordinate system e_1'', e_2'', e_3'' with $e_3'' = -\xi$ parallel to the dislocation line. The result is

$$c''_{ijkl} = c_{ijkl} - H\sum_{n=1}^{3}(S_{in}S_{jn}S_{kn}S_{ln} - \delta_{in}\delta_{jn}\delta_{kn}\delta_{ln}). \tag{29}$$

Here the rows of the orthogonal matrix $S = (e_1'', e_2'', e_3'')^t$ are the coordinates of the e_i'''s in the old orthonormal basis e_1, e_2, e_3. In these new coordinates, the elastic displacement field (u_1'', u_2'', u_3'') depends only on x_1'' and on x_2''. The dislocation line is oriented along $\xi = -e_3''$. In the new coordinates, the Burgers vector and the elastic displacement field satisfy $b_1'' = b_2'' = 0$ and $u_1'' = u_2'' = 0$ for a pure screw dislocation in an infinite medium. For a pure edge dislocation, $b_3'' = 0$ and $u_3'' = 0$. Secondly, the displacement vector (u_1'', u_2'', u_3'') is calculated as follows:

- Select three roots p_1, p_2, p_3 with positive imaginary part out of each pair of complex conjugate roots of the polynomial $det[a_{ik}(p)] = 0$, $a_{ik}(p) = c''_{i1k1} + (c''_{i1k2} + c''_{i2k1})p + c_{i2k2}p^2$.
- For each $n = 1, 2, 3$ find an eigenvector $A_k(n)$ associated to the zero eigenvalue for the matrix $a_{ik}(p_n)$.
- Solve $\mathrm{Re}\sum_{n=1}^{3} A_k(n)D(n) = b_k''$, $k = 1, 2, 3$ and $\mathrm{Re}\sum_{n=1}^{3}\sum_{k=1}^{3}(c_{i2k1}+c_{i2k2})A_k(n)D(n) = 0$, $i = 1, 2, 3$ for the imaginary and real parts of $D(1)$,$D(2)$,$D(3)$.
- For $k = 1, 2, 3$, $u_k'' = \mathrm{Re}[-\frac{1}{2\pi i}\sum_{n=1}^{3} A_k(n)D(n)\ln(x_1'' + p_n x_2'')]$.

Lastly, we can calculate the displacement vector u_k' in the non-orthogonal basis a_i from u_k''.

We use this strategy to calculate the elastic displacements of the perfect edge dislocation and pure screw dislocation in the case of gold. We have considered two straight dislocations: the perfect edge dislocation directed along $\xi = (1, -1, 2)/\sqrt{6}$ (with a Burgers vector which is one of the translation vectors of the lattice, and therefore glide of the dislocation leaves behind a perfect crystal [7]; and the pure screw dislocation along $\xi = (-1, -1, 0)/\sqrt{2}$. For the perfect edge dislocation, we select:

$$e_1'' = (-1, -1, 0)/\sqrt{2},\ e_2'' = (1, -1, -1)/\sqrt{3},\ e_3'' = (1, -1, 2)/\sqrt{6}, \tag{30}$$

which are unit vectors parallel to the Burgers vector $\mathbf{b}$, the normal to the glide plane $\mathbf{n}$, and minus the tangent to the dislocation line $-\xi$, respectively. For the pure screw dislocation, we have:

$$e_1'' = (1, -1, 2)/\sqrt{6},\ e_2'' = (-1, 1, 1)/\sqrt{3},\ e_3'' = (-1, -1, 0)/\sqrt{2}, \tag{31}$$

where e_2'' is a unit vector normal to the glide plane and e_3'' is a unit vector parallel to the dislocation line and to the Burgers vector (but directed in the opposite sense).

For gold, $C_{11} = 18.6$, $C_{44} = 4.20$, $C_{12} = 15.7$ and $H = 5.5$ in units of 10^{10} GPa. The lattice constant is $a = 4.08$ Å and the density is $\rho = 1.74$ g/cm^3. Figures 5 and 6 show the perfect edge dislocation and the screw dislocation obtained as stationary solutions of model (28). Their far fields match the corresponding elastic far fields of the dislocations (written in the non-orthogonal coordinates corresponding to the primitive cell vectors a_1, a_2, a_3). Dark and light colors are used to trace points placed in different planes in the original lattice. Note that the planes perpendicular to the Burgers vector in Fig. 5 have a two-fold stacking sequence 'dark-light-dark-light ...' The extra half-plane of the edge dislocation consists of two half planes (one dark and one light) in the dark-light-dark-light ... sequence. Movement of this unit dislocation by glide retains continuity of the dark planes and the light planes across the glide plane, except at the dislocation core where the extra half planes terminate [7].

5 CONCLUSIONS

We have proposed discrete models describing defects in crystal structures whose continuum limit is the standard linear anisotropic elasticity. The main ingredients entering the models are the elastic stiffness constants of the material and a dimensionless periodic function that restores the translation invariance of the crystal (and together with the elastic constants determines the dislocation size). For simple cubic crystals, their equations of motion with conservative dynamics are derived. Numerical solutions of these equations illustrate simple screw and edge dislocations. For fcc metals, the primitive vectors along which the crystal is translationally invariant are not orthogonal. Similar discrete models and equations of motion are found by writing the strain energy density and the equations of motion in non-orthogonal coordinates. In these later cases, we determine numerically stationary edge and screw dislocations.

This work has been supported by the MCyT grant BFM2002-04127-C02, and by the European Union under grant HPRN-CT-2002-00282.

REFERENCES

[1] F.R.N. Nabarro, *Theory of Crystal Dislocations*. Oxford University Press, 1967.

[2] J.P. Hirth and J. Lothe, *Theory of Dislocations, 2nd ed.* John Wiley and Sons, 1982.

[3] L. B. Freund, *Dynamic Fracture Mechanics*. Cambridge University Press, 1990.

[4] P. Szuromi and D. Clery, eds. *Special Issue on Control and use of defects in materials. Science* **281**, 939, 1998.

[5] E. Gerde and M. Marder. Friction and fracture. *Nature* **413**, 285–288 (2001).

[6] O. Rodríguez de la Fuente, M.A. González and J.M. Rojo. Ion bombardment of reconstructed metal surfaces: From two-dimensional dislocation dipoles to vacancy pits. *Phys. Rev. B* **63**, 085420-1–085420-11, 2001.

[7] D. Hull and D.J. Bacon. *Introduction to Dislocations, 4th ed.* Butterworth - Heinemann, 2001.

[8] O. Rodríguez de la Fuente, J.A. Zimmerman, M.A. González, J. de la Figuera, J.C. Hamilton, W.W. Pai and J.M. Rojo. Dislocation emission around nanoindentations on a (001) fcc metal surface studied by scanning tunneling microscopy and atomistic simulations. *Phys. Rev. Lett.* **88**, 036101-1–036101-4, 2002.

[9] N. W. Ashcroft and N. D. Mermin. *Solid State Physics*. Harcourt Brace College Pub., 1976.

[10] A. I. Landau. Application of a model of interacting atomic chains for the description of edge dislocations. *Phys. stat. sol. (b)* **183**, 407–417, 1994.

[11] A. Carpio and L.L. Bonilla. Edge dislocations in crystal structures considered as traveling waves of discrete models. *Phys. Rev. Lett.* **90**, 135502-1–135502 -4, 2003.

[12] L.D. Landau and E.M. Lifshitz, *Theory of elasticity, 3rd ed.* Pergamon Press, 1986.

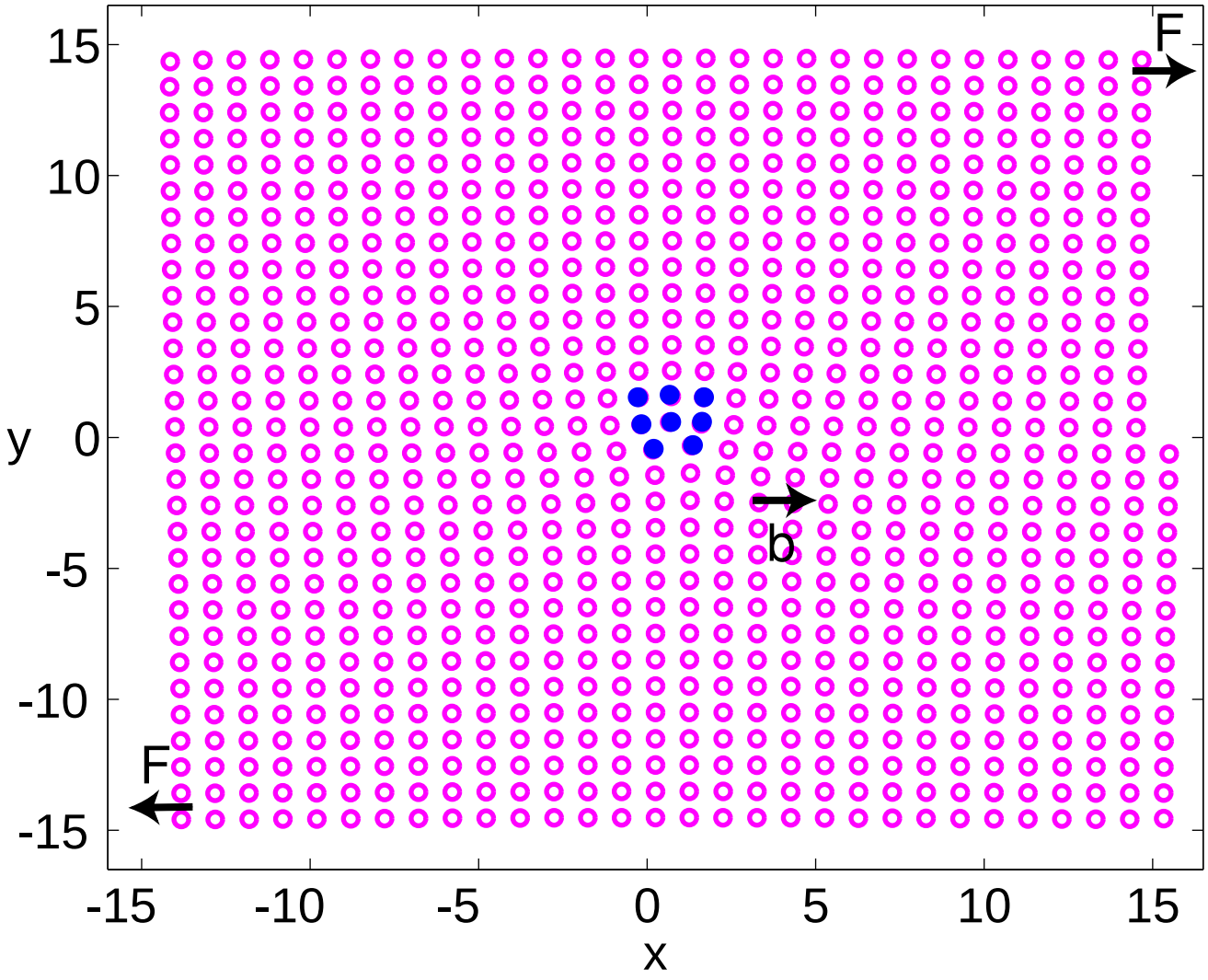

Figure 1: Deformed cubic lattice in the presence of an edge dislocation for the piecewise linear $g(x)$ of Eq. (8) with $\alpha = 0.1$.

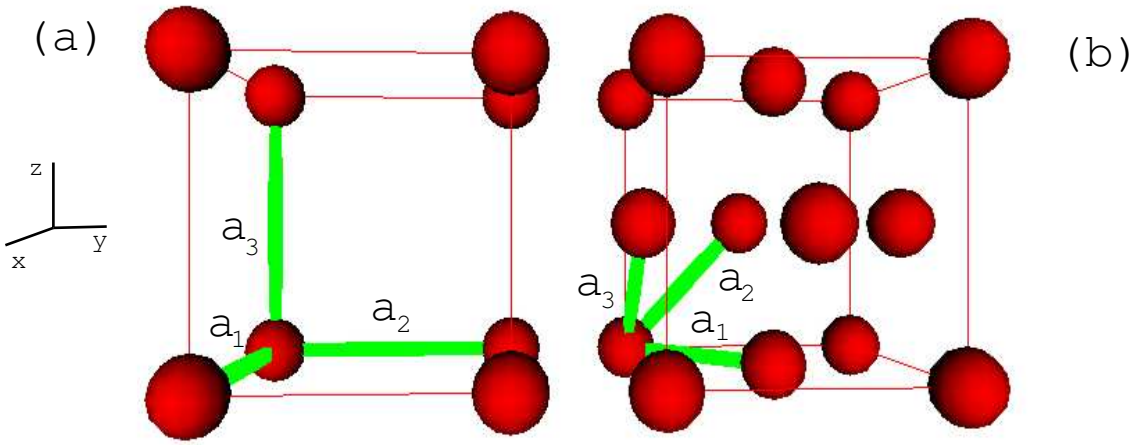

Figure 2: Reference systems spanned by: (a) three primitive vectors of the simple cubic lattice, (b) three primitive vectors of the face centered cubic lattice.

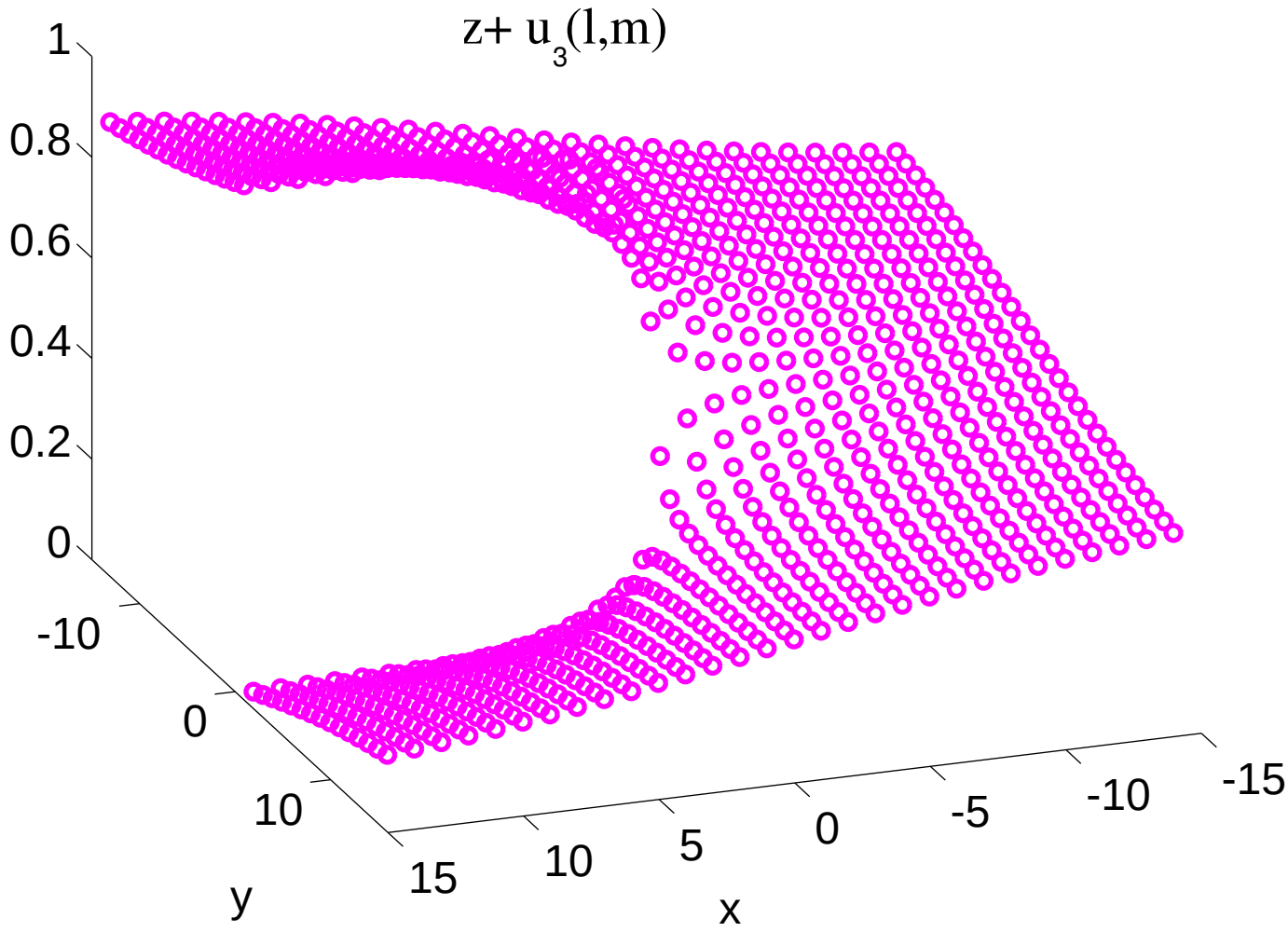

Figure 3: Screw dislocation for the piecewise linear $g(x)$ of Eq. (8) with $\alpha = 0.1$.

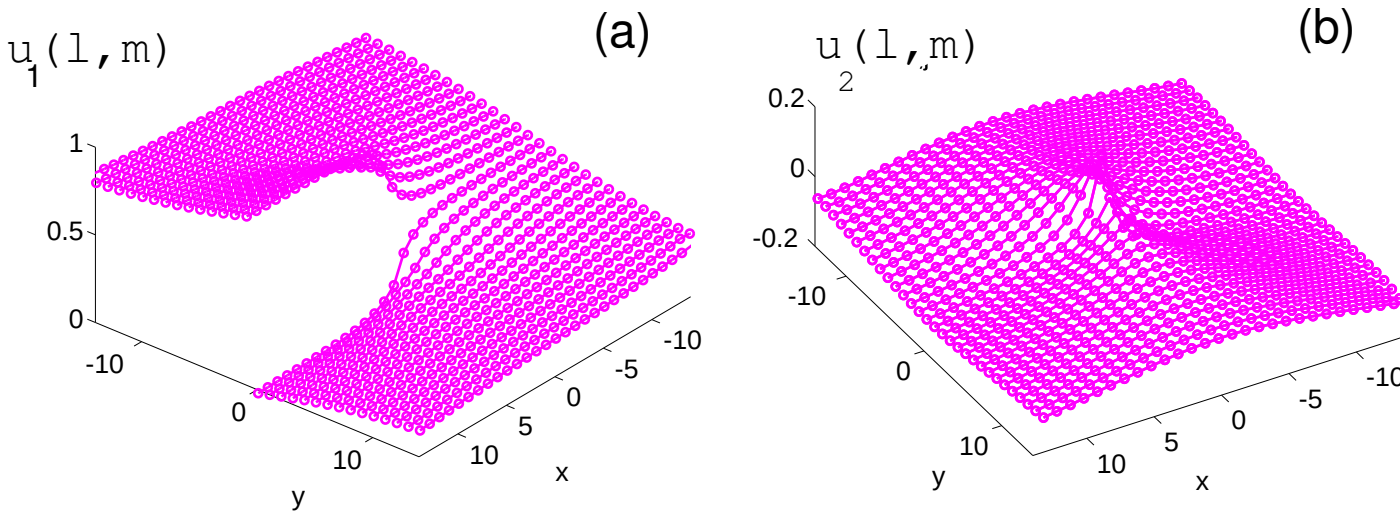

Figure 4: Profile of an edge dislocation for the piecewise linear $g(x)$ of Eq. (8) with $\alpha = 0.1$: (a) $u_1(l,m)$, (b) $u_2(l,m)$.

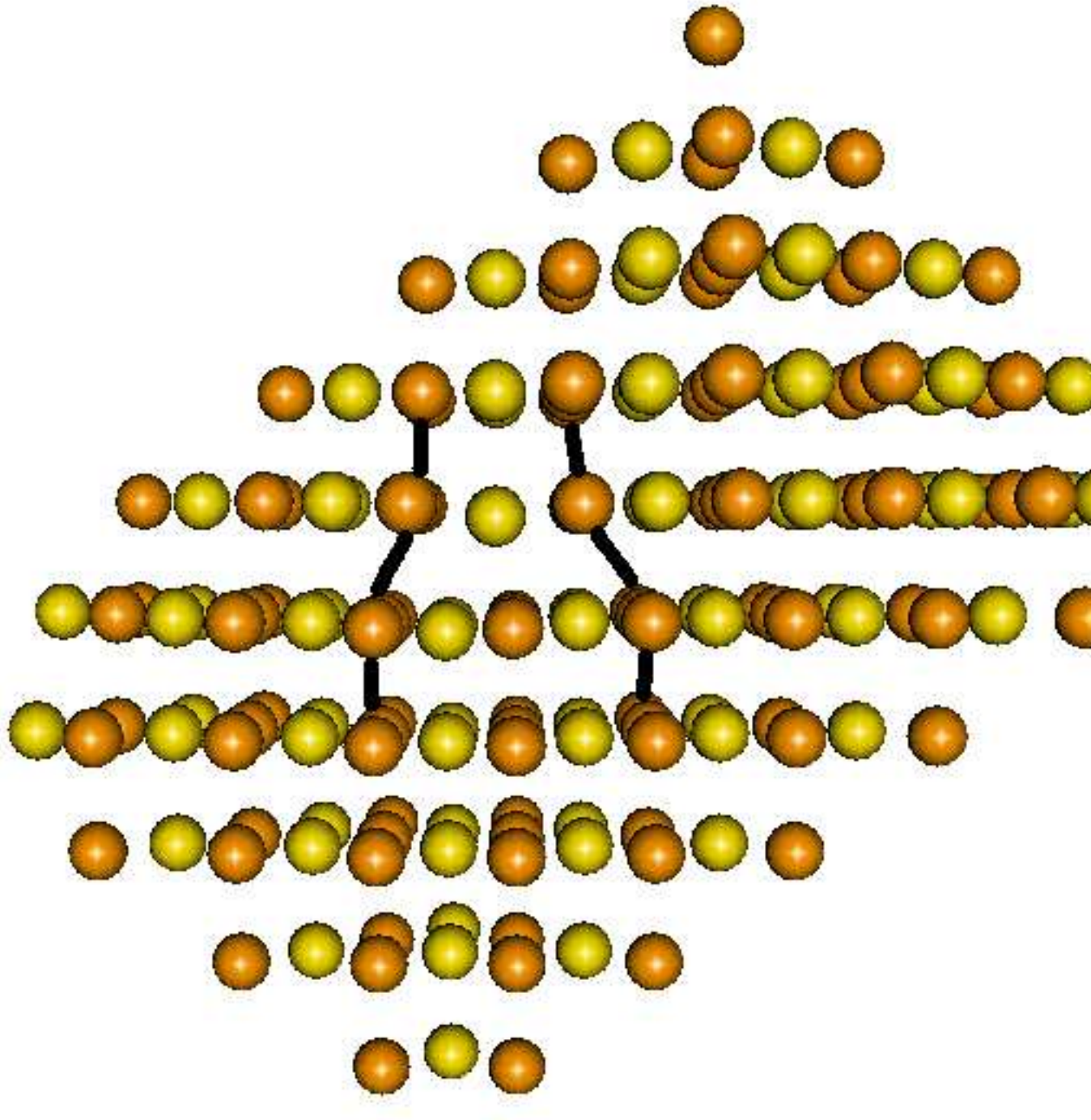

Figure 5: Perfect edge dislocation in a gold lattice displaying a two-fold stacking sequence of planes containing dark and light atoms. The dislocation line is perperdicular to the paper.

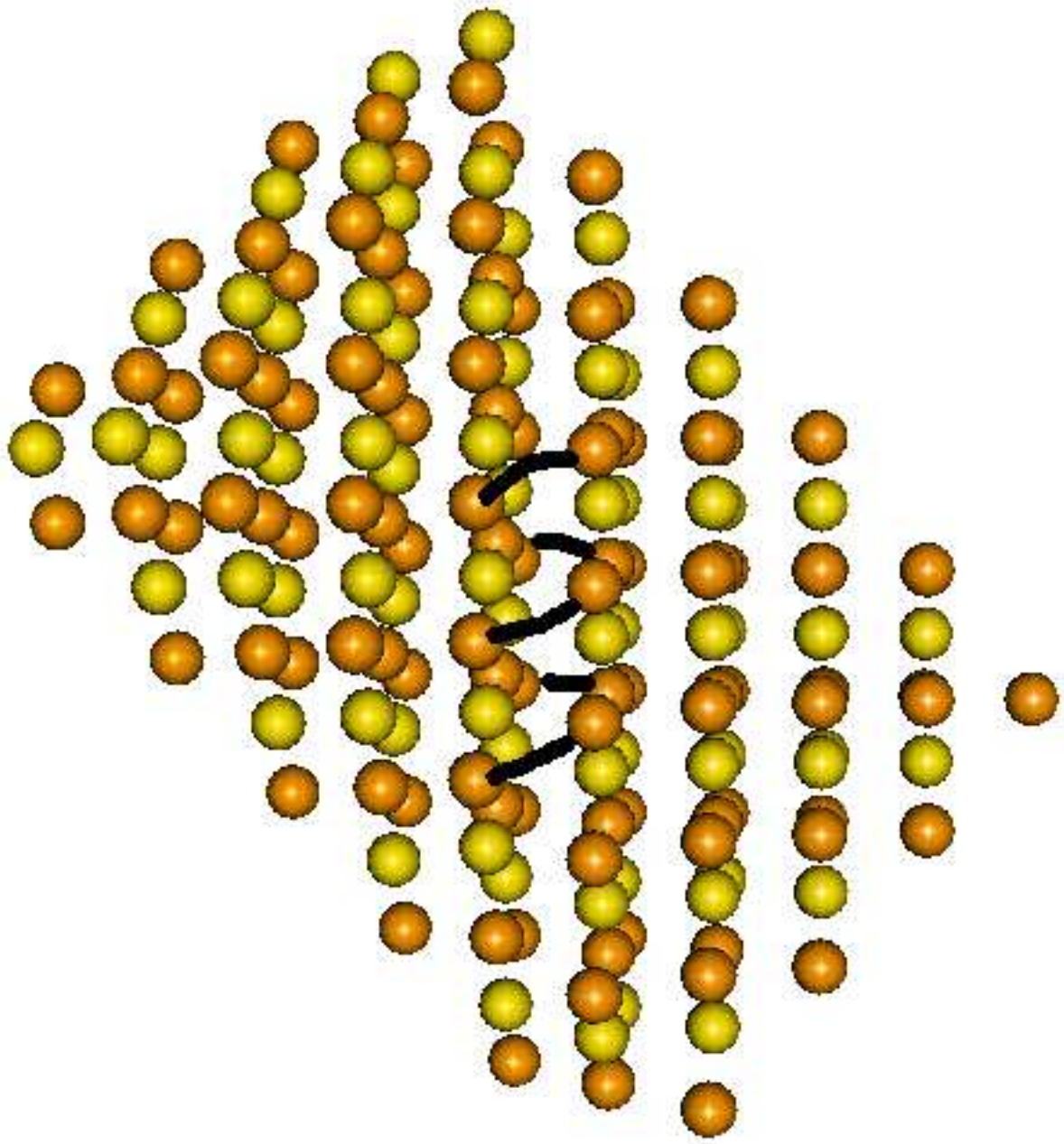

Figure 6: Screw dislocation in a gold lattice. The dislocation line is parallel to the z axis.